Biomacromolecules

Anatolian University Libraries Consortium anakos

Subscriber access provided by HACETTEPE UNIVERSITESI KUTUPHANESI

Article

High-Affinity Copolymers Inhibit Digestive Enzymes by Surface Recognition

Patrick Gilles, Kirstin Wenck, Inga Stratmann, Michael Kirsch, Daniel A. Smolin, Torsten Schaller, Herbert de Groot, Arno Kraft, and Thomas Schrader

Biomacromolecules, **Just Accepted Manuscript** • DOI: 10.1021/acs.biomac.7b00162 • Publication Date (Web): 18 Apr 2017

Downloaded from http://pubs.acs.org on April 24, 2017

Just Accepted

"Just Accepted" manuscripts have been peer-reviewed and accepted for publication. They are posted online prior to technical editing, formatting for publication and author proofing. The American Chemical Society provides "Just Accepted" as a free service to the research community to expedite the dissemination of scientific material as soon as possible after acceptance. "Just Accepted" manuscripts appear in full in PDF format accompanied by an HTML abstract. "Just Accepted" manuscripts have been fully peer reviewed, but should not be considered the official version of record. They are accessible to all readers and citable by the Digital Object Identifier (DOI®). "Just Accepted" is an optional service offered to authors. Therefore, the "Just Accepted" Web site may not include all articles that will be published in the journal. After a manuscript is technically edited and formatted, it will be removed from the "Just Accepted" Web site and published as an ASAP article. Note that technical editing may introduce minor changes to the manuscript text and/or graphics which could affect content, and all legal disclaimers and ethical guidelines that apply to the journal pertain. ACS cannot be held responsible for errors or consequences arising from the use of information contained in these "Just Accepted" manuscripts.

ACS Publications

Biomacromolecules is published by the American Chemical Society. 1155 Sixteenth Street N.W., Washington, DC 20036

Published by American Chemical Society. Copyright © American Chemical Society. However, no copyright claim is made to original U.S. Government works, or works produced by employees of any Commonwealth realm Crown government in the course of their duties.

High-Affinity Copolymers Inhibit Digestive Enzymes by Surface Recognition

Patrick Gilles,[‡] Kirstin Wenck,[‡] Inga Stratmann,[‡] Michael Kirsch,[†] Daniel A. Smolin,[‡] Torsten Schaller,[‡] Herbert de Groot,[†] Arno Kraft,[§] Thomas Schrader[‡]*

[†]University of Duisburg-Essen, Faculty of Medicine; [‡]University of Duisburg-Essen, Faculty of Chemistry, Universitaetsstr. 7, 45117 Essen, Germany; [§]Heriot-Watt University, Edinburgh, Scotland, UK EH14 4AS

KEYWORDS. Proteases, Hydrolases, Enzyme Inhibition, Supramolecular Chemistry, Radical Copolymerization

ABSTRACT.
This account presents a general method for the construction of polymeric surface binders for digestion enzymes. Two prominent parts, namely the modification of the copolymer composition and the screening assay for the most powerful inhibitors are both amenable to parallelization. The concept hinges on the appropriate selection of amino-acid-selective comonomers, their free radical copolymerization, and subsequent screening of the resulting copolymer library for efficient enzyme inhibition. A microscale synthetic procedure for the copolymerization process was developed, which produces water-soluble affinity polymers that can be stored for years at room temperature. Initial parallel screening was conducted in standard enzyme assays to identify polymeric inhibitors, which were subsequently subjected to determination of IC_{50} values for their target enzyme. For all digestion enzymes except elastase a number of polymer inhibitors were found, some of which were selective towards one or two protein targets. Since the key monomers of the best inhibitors bind to amino acid residues in the direct vicinity of the active site, we conclude that efficient coverage of the immediate environment by the copolymers is critical. Strong interference with enzymatic activity is brought about by blocking the substrate access and product exit to and from the active site.

Introduction.

Many proteins operate by the same common mechanism and hence share very similar active sites. Thus, serine proteases all contain the catalytic triad Asp-His-Ser and an oxyanion hole, and achieve specificity mainly through additional binding pockets for their substrates. The classical approach for the development of potent enzyme inhibitors involves rigid substrate mimetics

which carry tailored substituents for the optimal filling of specificity pockets. A very elegant example is the development of a thrombine inhibitor in the *Diederich* group, which occupies the S1-, D- and P-pocket and thus achieves very high affinity and thrombin/trypsin selectivity.[1] The preparation of this low-molecular-weight drug, however, requires a multistep enantio-selective synthesis. Moreover, if an enzyme does not offer large pockets, which are characteristic in shape and charge distribution, the development of enzyme-specific active site inhibitors becomes problematic.

In those cases it would be advantageous to overcome the limitation of active site targeting and include the protein surface for molecular recognition and inhibition. Quite often the size, topology and amino acid distribution of similar serine proteases differ greatly and create opportunities for their selective inhibition. In this respect the development of linear, branched or cross-linked affinity copolymers is an attractive approach, because these can provide large surface areas and offer a number of different binding sites within one molecule, exploiting the concept of multivalency and hetero-avidity.[2] If surface recognition is thus combined with steric hindrance to the entrance of the active site, a selected enzyme will stop to process its substrate. Such a supramolecular inhibition mode will be reversible in the presence of a competitor. However, it requires multipoint binding of the copolymer on the enzyme surface.

Various new concepts have evolved in recent years which focus on tailored dendrimers and polymers for protein surface recognition: *Haag* developed dendrimeric polyglycerol sulfates (dPGS) for multivalent Selectin binding on leukocytes for the control of viral in-fections.[3] Chiral ruthenium(II) trisbipyridine complexes with up to six L-aspartyl side chains in the ligand have been found to bind to the active site of proteases, making it possible to inhibit chymotrypsin with high efficiency. *(Wilson, Ohkanda)*.[4-5] Detection and identification of proteins has been accomplished with nanoparticle–fluorescent polymer 'chemical nose' sensors *(Rotello)*, whereas *s*elective sensing of metallo-proteins could be achieved from nonselective binding using a fluorogenic amphiphilic polymer *(Thayumanavan)*.[6-7]

Lightly crosslinked nanoparticles recognize protein surfaces and exploit multivalency of unspecific noncovalent attraction (*Shea*).[8] Molecularly imprinted hydrogels add the template-effect in order to achieve improved affinity and selectivity *(Haupt et al.)*.[9] Inspired by this pioneering work, core-shell particles were developed, which combine immobilization of an anchor monomer and self-assembly of the protein template *(Zhang)*.[10] Various new methods have been recently developed, exploiting the concept of molecular imprinting by peptidic and protein templates.[11-15] However, all these approaches have hitherto been limited to conventional monovalent binding monomers and lack the element of specific molecular recognition.

Our group adds the following supramolecular component: over the past years, we have designed a large variety of amino acid-selective binding monomers. A simple conventional radical copolymerization of selected monomers gives access to new water-soluble materials which

display high affinities through multivalency[16] and surprising protein specificity by cooperative binding of the appropriate functional monomers.[17] Molecular recognition of characteristic amino acid residues on the surface of lysozyme then leads to efficient enzyme inhibition, which can be switched on and off.[18] Very recently we could show that the correct monomer choice also allows epitope-selective binding, e.g. of the Fc part in IgGs.[19]

Serine proteases are digestion enzymes which operate in the intestines and provide a challenging medicinally relevant target. Their upregulation inside the pancreas after shock, during cardiac surgery or organ transplants can lead to ischemia and reperfusion lesions.[20] These in turn may cause acute pancreatitis, a life-threatening emergency.[21] Trypsin holds a key role because it activates other hydrolases whose uncontrolled action may ultimately damage multiple organs.[22] Treatment of such a condition with anti-secretory hormones[23] or protease inhibitors is unsatisfactory, most likely because most of them act unspecifically on proteases of similar structure.[24]

Experimental Section.

Materials. All reagents and proteins were used as received. Trizma Base, BAPNA, dodecylamine were purchased from Fluka (Buchs, Switzerland), dry solvents from Acros Organics (geel, Belgium), H-Lys(Z)-OtBu HCl from Bachem (Bubendorf, Switzerland) and deuterated solvents were purchased from Deutero (Kastellaun, Germany). All other chemicals were purchased from Sigma Aldrich (Steinheim, Germany).

Methods. *Nuclear Magnetic Resonance (NMR).* ^{1}H and ^{31}P spectra were recorded with a Bruker DMX 300, further ^{1}H and ^{13}C spectra were recorded with a Bruker DRX 500 using deuterated solvents. Residual solvent peak was used as an internal standard for peak calibration.

Size Exclusion Chromatography (SEC). Polymer molecular weights were determined by size exclusion chromatography with a JASCO PU-980 pump and refractive index detector RI-930. For cationic polymers two consecutive PSS NOVEMA Max 300 x 80 mm columns (PSS, Mainz, Germany) were used. Anionic polymers were characterized over two consecutive PSS HEMA Bio linear 300 x 80 mm columns (PSS, Mainz, Germany). As standards pullulanes with different molecular weights were used (PSS, Mainz, Germany).

Mass spectrometry. Mass spectra were recorded with a Bruker maXis 4G and with a Bruker BioTOF III time of flight mass detector with ESI ion source.

Isothermal Titration Calorimetry (ITC). ITC measurements were recorded with a VP-ITC calorimeter from MicroCal.

Lyophylization. Synthesized polymers were lyophilized using a device from Christ, Model Alpha 2-4 LSC.

UV/Vis and fluorescence spectroscopy. The absorption spectra were recorded with a Tecan Infinite M200 Microplates reader. The used Non-Tissue Culture-Treated Plate, 96-well, flat bottom with low evaporation lid (polystyrene) purchased from BD Falcon.

Parallel copolymerization. For the parallel polymerization a HLC-Heating MHL 23 thermomixer from Ditabis were used.

General procedure for the parallel free radical copolymerization. Stock solutions of all monomers were degassed according to the „freeze-and-exhaust" method. Under argon these solutions were transferred into a 2 mL polymerization vessel and 5 mol % AIBN were added. The resulting total volume never exceeded 1300 µL. Subsequently the polymerization was conducted in a thermomixer at 70 °C und 600 rpm. After 24 - 30 h the polymerization solutions were transferred to a small conical shaped flask and subjected to lyophilization.

The resulting residue was dissolved in little water and transferred into a small centrifugal filter unit (Amicon Ultra 2mL 3K Ultracel - 3K Membrane, Millipore). Ultrafiltration was carried out three times at 4000 rpm for 60 min, then a fourth ultracentrifugation followed at 4000 rpm for a total of 100 min using a Eppedorf Centrifuge 5706. The resulting oligomer- and monomer-free solution was subsequently transferred into a 2mL Eppendorf tube and subjected again to lyophilization. The voluminous colorless lyophylizate was further examined: NMR spectra indicated the degree of conversion and the stoichiometric ratio of comonomers inside the final copolymer. SEC was used for the molecular weight determination of the polymers.

Enzyme assays. *General remarks.* All substrate and enzyme solutions were freshly prepared and stored at 0°C during the measurements. Stock solutions of copolymers had a mass concentration of 20 mg/mL in doubly distilled water. Measurements were conducted in 96-well microplates. Before each assay, absorption spectra of substrate, enzyme and chromophore were obtained, in order to determine the absorption maximum of the chromophore and to secure that absorption of enzyme and substrate was negligible at the selected wavelength.

In order to validate each method, a known reference inhibitor was tested, its IC_{50} value was determined and compared to the literature value. Subsequently, a screening was conducted in triplicate with all polymers. Each NTA-containing polymer was measured in the absence and in the presence of 50 mol-% Ni^{2+} ions with respect to the NTA amount within the polymer. If an inhibitory effect was observed for a polymer within the error limits of the screening, its IC_{50} value was subsequently determined. To this end, the enzyme velocity was measured for 10 different polymer concentrations; each experiment was carried out in triplicate (see more details in the Supporting Information).

Results and Discussion.

We asked ourselves whether or not it would be possible to design a synthetic polymer which would be capable of distinguishing, e. g., between trypsin and chymotrypsin and lead to efficient inhibition simply by binding to the protein surface? Thus we embarked on a program aimed at the discovery of highly specific polymeric inhibitors for disease-relevant proteases (**Fig. 1**). For economic reasons, this required the development of a general method for the parallel synthesis of affinity copolymers in small amounts. In addition, we needed to probe their interaction with digestion enzymes. This was realized in three stages: synthesis of new binding monomers, development of a small scale combinatorial polymerization, and an assay for the parallel screening of target enzymes.

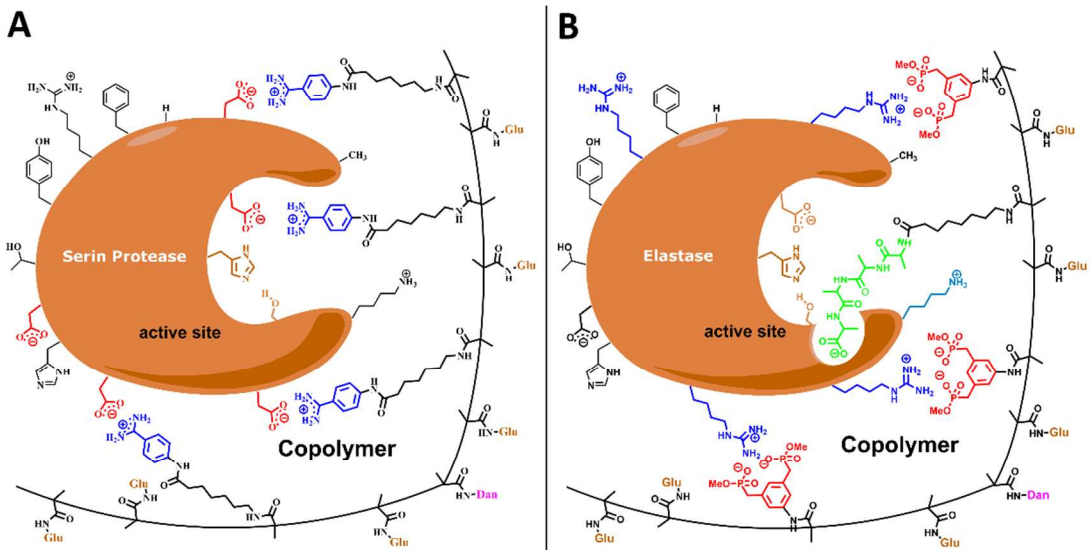

Figure 1. Schematic representation of linear affinity copolymers recognizing the surface of serine proteases. **A** A benzamidine comonomer binds to aspartates and glutamates on the surface and within the active site. **B** A bisphosphonate comonomer selectively recognizes arginines on the protein surface – it is supported by an anchor monomer with a terminal alanine unit filling the specificity pocket of elastase.

For this study we chose a representative series of seven digestive enzymes involved in pancreatitis and intestinal injuries. Inspection of all protein surfaces revealed very different sizes, topologies and amino acid compositions - ideal to test the polymers' potential to distinguish between protein surfaces within the same family of enzymes. **Table 1** displays the protein sizes and charges together with their main cleavage sites and typical inhibitors.

Protein	Mechanism	Amino Acid Residues	MW [kD]	pI	pH Optimum	Inhibitor	Cleavage Site

Elastase	Serine protease	**240**	**26**	**8.8**	**8.5**	α1-Antitrypsin	Ala, Gly
α-Chymotrypsin	Serine protease	**241**	**25**	**8.7**	**7.8**	Aprotinin	Phe, Tyr, Trp
Trypsin	Serine protease	**233**	**24**	**10.1**	**7.5-8.5**	*p*-Amino-benzamidine	Arg, Lys
Carboxypeptidase A	Zinc protease	**307**	**35**	**6.0**	**7.5**	Benzomercapto -propanoic acid	Phe, Trp, Leu
Kallikrein	Serine protease	**619**	**86**	**4.5**	**7.0-8.0**	Aprotinin	Arg
Thrombin	Serine protease	**308**	**37**	**7.2**	**7.5-8.5**	Argatroban	Arg
Cathepsin D	Aspartate protease	**346**	**48**	**6.0**	**3.5-5.0**	Pepstatin A	Phe-Phe

Table 1. Overview of seven selected digestion enzymes for pancreatitis and intestinal injury, illustrating their diverse sizes, charges and pI values.

Binding monomers. For each major class of amino acid residues we developed a series of methacrylamides which carry a specific binding site - the current status of this library is presented in **Scheme 1**: Lysine and arginine are recognized by a methacrylamide-based bisphosphonate dianion (BP, C5-BP, C6-BP); serine, threonine as well as diols in glycosylated proteins can form cyclic esters with aminomethylphenylboronic acid units (Bor), whereas non-polar amino acids can interact with cyclohexyl or dodecyl methacrylamides (Dod, C6-CyH). Further inclusion of a glucosamine-based monomer (Glu) is beneficial because it greatly enhances water solubility, and a dansyl moiety (Dan) provides a fluorescence label for convenient detection in titration or microscopy experiments.

In order to complete the series, several new binding monomers were synthesized for acidic amino acids, aromatic amino acids and histidine. A guanidiniocarbonylpyrrole, previously introduced by *Schmuck et al.* as a powerful aspartate and glutamate receptor[25] was converted into a polymerizable methacrylamide CBS. For improved steric accessibility, the bisphosphonate monomers C_5-Sp and C_6-Sp were generated with a C_5 and C_6 spacer. Finally, Ni^{2+} complexation of the nitrilotriacetic acid headgroup converted NTA and NTA-Glu into monomers for histidine recognition.[26] In an attempt to further improve specificity to the protein-selective polymers, we also synthesized methacrylamides of amino acids which can occupy the S1-pocket, but avoided C-terminal functionalization of the monomers as carboxyamides in order to prevent their proteolytic cleavage. A benzamidine methacrylamide was used as an anchor monomer for Trypsin as mentioned by *Haupt* et al. Similar to the BP unit, several other key monomers for unpolar and charged residues (BP, BA, CyH, ED) were also prepared with a C_5- or C_6- spacer between receptor unit and methacrylamide, in order to facilitate their interaction with remote amino acid residues on the protein surface.

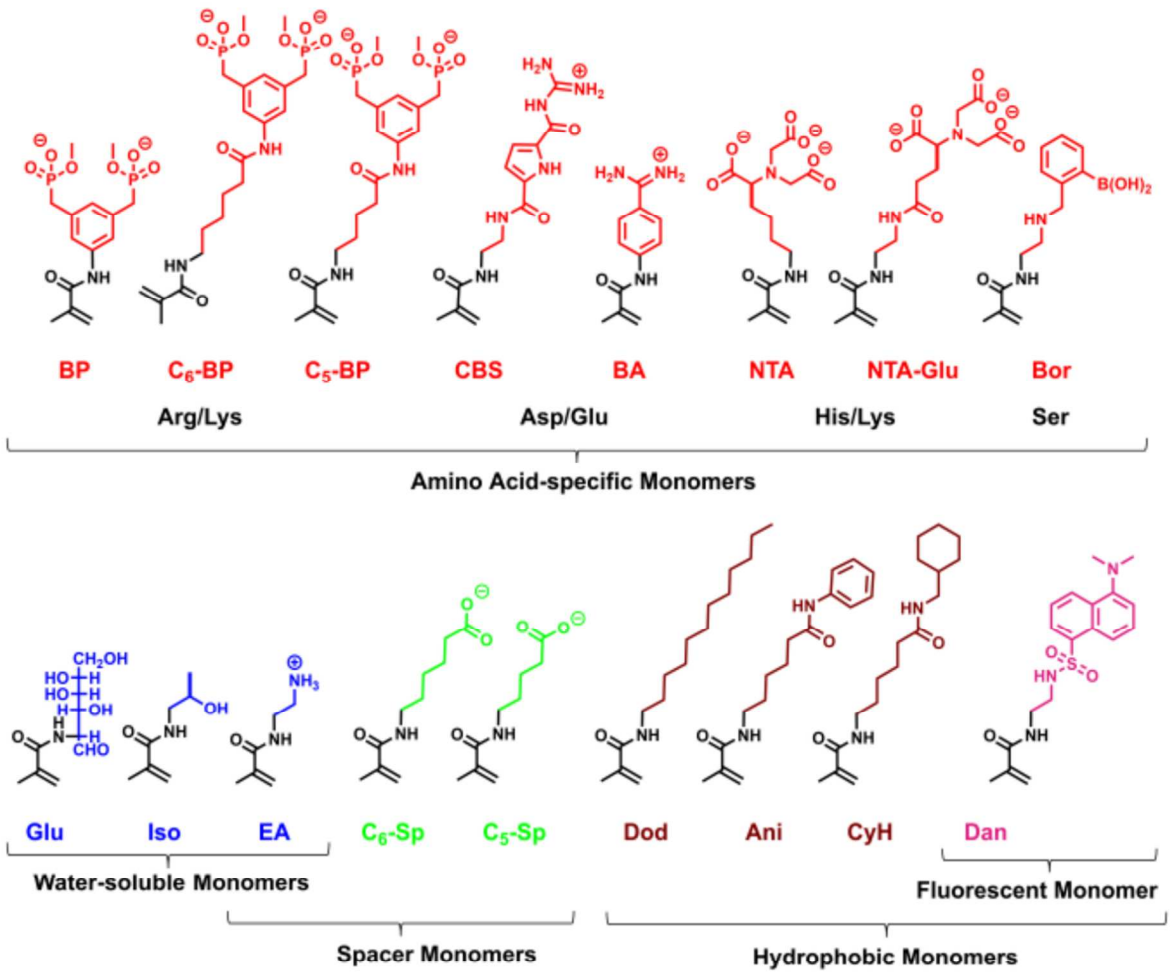

Scheme 1. Methacrylamide-based comonomer pool for the main classes of amino acids and special monomers. BP = Bisphosphonate; CBS = Guanidiniocarbonylpyrrole; BA = Benzamidine; NTA = Nitrilotriacetic acid; Bor = Boronic acid; Glu = Glucosamide; Iso = Amidoisopropanol; EA = Ethyleneamine; Sp = Spacer; Dod = Dodecyl; Ani = C_6-Anilide; CyH = Cyclohexyl; Dan = Dansyl.

The synthetic pathways towards the main new compounds are depicted in **Scheme 2.** Briefly, guanidiniopyrrole carboxamide as a powerful carboxylate binding site (CBS) was generated from an *N*-Boc benzyl ester precursor, hydrogenated and coupled with ethylenediamine mono-methacrylamide (EA); mild Boc removal was effected with HCl in dioxane.

A bisphosphonate nitroarene precursor was reduced to the respective aniline, and subjected to amide coupling with C_5-SP or C_6-SP. Subsequent mild dealkylation with LiBr furnished the extended spacer monomers C_5-BP and C_6-BP. A modified procedure was used to prepare the NTA building block: 2 equivs. of *O-t*-butyl-bromoacetate attached to the primary α-amine in the

mixed tBu/Bn glutamate diester, debenzylated and coupled with excess EA. Mild removal of all Boc groups yielded NTA-Glu.[27]

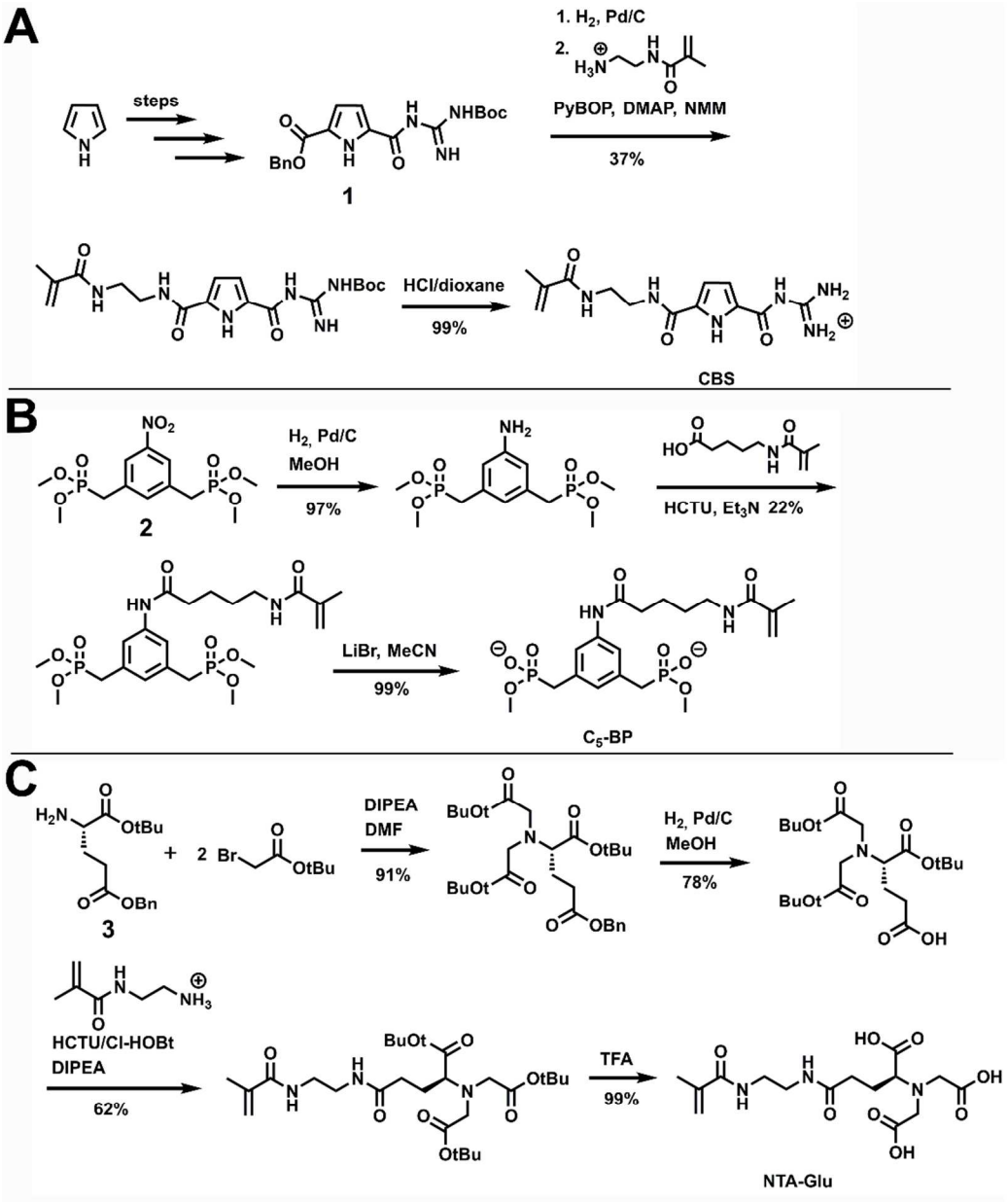

Scheme 2. Synthetic routes to three new comonomers for charged amino acid residues: **A** guanidiniocarbonylpyrrole carboxamide monomer CBS, **B** extended bisphosphonate monomer C_5-BP and **C** nitrilotriacetic acid comonomer NTA-Glu.

Parallel copolymerization. In order to avoid polymer-analogous reaction steps which often suffer from incomplete conversion, free monomers were used without protecting groups. All monomers were soluble in water, DMF or mixtures thereof.

Copolymerization of ternary mixtures of comonomers of different size and polarity strongly depends on monomer reactivity ratios.[28] To confirm that all key binding monomers are readily incorporated into a copolymer, we carried out a simple copolymerization experiment in an NMR tube. A 1:1:1 mixture of a charged monomer (BP), a polar neutral monomer (Glu) and a non-polar monomer (C_6-CyH) was dissolved in D_2O together with a radical initiator (AIBN), degassed and heated to 70 °C for 96 hours. ^{1}H NMR spectra were recorded before and throughout the polymerization. The decrease in the integrals of the alkene signals (relative to the aromatic signals) was followed over time. The dianionic bisphosphonate was more slowly incorporated than the other two monomers (**Fig. 2**), most likely due to electrostatic repulsion. Obviously, the BP likes to be surrounded by less polar monomer units, which in turn prefer formation of homopolymer spacer fragments. The resulting isolation of binding monomer units supports their specific interaction with amino acid binding partners on the protein surface.

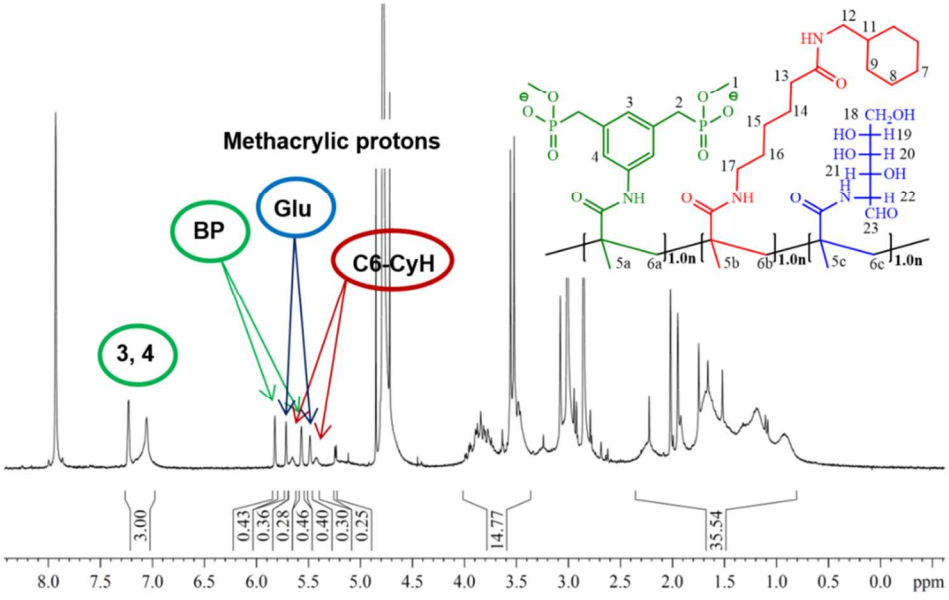

Figure 2. Determination of relative copolymerization kinetics from ^{1}H NMR spectroscopic monitoring of the monomer consumption starting with a ternary 1:1:1 mixture BP/Glu/C6-CyH (300 MHz in D_2O).

Further optimization revealed optimal copolymerization conditions for 24 h at 70 °C with good reproducability. Each monomer was kept in a DMF/water stock solution at a concentration of ~ 100 mg/mL; prior to the copolymerization, the monomer solutions were freshly degassed and transferred with an Argon-filled syringe into a small dry 2 mL vial, which also contained a known amount of AIBN (usually 5 mol%). Maximum solvent loading was 2 mL per vial, maximum monomer loading was 100 mg. All copolymerizations were carried out in clear solutions of aqueous DMF. After sealing with glass stopcocks, 24 vials were placed on a thermomixer and were gently shaken for 24 h at 70 °C. During this time, copolymerization was complete. The solvent was evaporated to dryness and the residue was lyophilized to give an almost colorless amorphous solid.

NMR spectra of the crude products revealed the presence of small amounts of DMF and monomers, which were subsequently removed by ultrafiltration through centrifugal filters.[29] Final lyophilization afforded colorless voluminous solids of pure material in overall yields around 50%.

Almost all new polymeric inhibitors proved to be water-soluble; copolymers containing the CBS unit with its guanidiniopyrrole cation required 2-3 equivs. of ethyleneamine (EA) monomer or 10 equivs. of glucosamine (Glu) monomer to be sufficiently soluble in water. They were examined by size exclusion chromatography (SEC) in neutral aqueous solution at a concentration of 1 mg/mL. Poly(ethylene glycol) standards were used for calibration and produced Number-average molecular weights between 35 kD and 200 kD. Since the PEG skeleton bears little structural similarity to methacrylamides, calibration with polyacrylates was also attempted, but produced higher molecular weights with irregular large deviations, even for polymers with comparable composition. Polydispersities (PDI) or M_w/M_n ratios were between 2 and 3 as expected from conventional radical copolymerization.

Finally, as a purity check, each filtered polymer was examined by ^{1}H NMR spectroscopy in order to determine the content of rest monomer; evaluation of the integrals for the sharp methacrylamide peaks usually remained below 1 mol-%. Integration of broad polymer peaks was sometimes problematic; it was, however, essential to determine copolymer composition. Usually, only 5% less of charged comonomers were built into the copolymers, especially if the mixture contained large amounts of the glucose monomer. ^{31}P NMR spectra of all phosphonate-containing copolymers just displayed a broad singlet at 23.7 ppm.

Table 2 gives a survey of over 50 purified copolymers, 49 of which were water soluble. Structurally related copolymers are shown as small series which could be used to study the contributions of specific comonomer binding sites to the overall recognition event. The number of glucosamide equivalents (1.0 – 5.0) necessary for water solubility directly reflects the content of nonpolar monomer units. In some dodecyl-containing polymers (P05, P13 and P41) the aliphatic protons were invisible in the ^{1}H NMR spectrum, and aqueous solutions appeared blurred, pointing to self-assembly into micellar aggregates. Attempted formation of zwitterionic polymers was successful for P30, which combined BP and CBS monomers and produced clear solutions in aqueous buffer, which showed the characteristic signals for both comonomers. In general, copolymerization results were reproducible, as exemplified in three cases by comparison of NMR spectra as well as SEC parameters (M_n and PDI).

Table 2. List of all affinity copolymers with their exact compositions and molecular weights.

Polymers	Monomer Building Blocks (in eq.)																	M_n [kDa]
	CBS	CBS-Boc	BA	BP	5'-BP	6'-BP	NTA	NTA-Gl	Bor	Ani	6'-CyH	Dod	Glu	Iso	ED	C_6-Sp	Dan	
P01				3				1					1				0.5	135
P02				2				1					1					139
P03				1.5						0.5			1					122
P04				1.5							0.5		1					133
P05				1.5								0.5	1					150
P06				1.5									1			0.5		158
P07				3						1			1	1				132
P08				1				1		1			1					122
P09				1				1			0.5		1					142
P10				1				1					1				0.3	145
P11				1						0.5			1	1		0.3		133
P12				1							0.5		1	1		0.3		132
P13				1								0.5	1	1			0.3	124
P14	1												3	1	1			133
P15									1	0.5					3			123
P16									1			0.5			3			81
P17									1		0.5				3			78
P18				4					1									116
P19								0.5				0.5	1	1				71
P20								0.5					1	1		0.5		118
P21				1				0.5					1	1		0.5		158
P22			1								1		3					196
P23			1										3				1	202
P24			1							1			3					107
P25			1										1	1				142
P26	1												3					180
P27	1										1		4					147
P28	1		1										4					167
P29	1												5				1	148
P30	1			1									3					123
P31		1		1									3					87
P32				4			1		0.5									134
P33							4										1	-
P34				4													1	120
P35			1										1					222
P36				1														103
P37				1						1		1						155
P38													1					37
P39				3			1						1				0.5	100
P40				3			1						1					94
P41				5								1	0.3				0.4	103
P42							1											112
P43				1			3						1					83
P44				2			2						1					92
P45				3			1						1					104
P46				3			1						1				1	119
P47				1.5	1.5		1						1					104
P48				1.5		1.5	1						1					118
P49					3		1						1					95
P50						3	1						1					113
P51									1						2		0.3	67
P52				5								1	1					73

It should be noted, that no evidence of aggregate formation was obtained for any of the copolymers, such as, e. g., excessive broadening of NMR signals or turbidity of solutions. Very recent DLS as well as DOSY measurements indicated hydrodynamic radii corresponding to nonaggregated species. Moreover, to avoid aggregation, the composition of all copolymers had at least 65% of highly water-soluble functional groups.

In Table 2 the different series of copolymers with a common major binding monomer are presented in groups. From top to bottom: P01-P13 all contain the bisphosphonate monomer BP and are therefore negatively charged. Within this large group, three subgroups represent combinations with nonpolar monomers Ani, C_6-CyH and Dod: P03-05, P07-10 and P11-13. The next major series comprises P14-17 which share the cationic ethyleneamine unit EA. Strongly overlapping is the series P15-27 which all carry the boronic acid moiety Bor. P19-21 contain the negatively charged NTA unit. With P22-26, a series of cationic benzamidine-containing polymers (BA) is introduced, followed by P26-31, presenting the positively charged CBS unit. P39-P36, P38 and P42 are all homopolymers or polymers with only one amino acid recognition unit, namely with NTA, BP, BA or Glu monomers. Finally, P42-P50 are all NTA-based copolymers, the first of them (P43-P46) rich in BP, the next subgroup (P47-P50) rich in BP with spacers.

Parallel enzyme assays. These polymer materials were subsequently used directly to investigate their interaction with proteolytic enzymes. Since determination of protein affinities by titration methods is very time-consuming, and does not necessarily coincide with inhibitory power, a parallel screening method was developed which measured the attenuation of enzymatic activity. To this end, a 10-fold molar excess of each polymer was incubated with the respective enzyme and treated with excess substrate. From the relative decrease in enzyme velocity the best inhibitors were selected for a subsequent determination of their IC_{50} values (**Figure 3**). All titrations were done at physiological pH and ionic strength.

Standard enzyme assays were established which used typical peptidic enzyme substrates whose proteolytic cleavage produced or consumed a colored product with a strong absorption in the visible range of the electromagnetic spectrum.[30] For each enzyme assay UV-vis spectra confirmed the absorption maximum of the released chromophore and ascertained that enzyme as well as substrate absorption at the selected wavelength were negligible. Almost all enzyme assays were cross-checked by determination of the IC_{50} value of a known reference inhibitor, whose literature value was reproduced. Buffers (Trizma, Hepes) were adjusted to optimal pH for each enzyme (5.0 and 7.4 - 8.0), and contained physiological salt concentrations.

Elastase[31] (PDB code 1H1B, 2Z7F) is a serine protease, produced in zymogenic form in the exocrinic part of the pancreas, and activated by trypsin cleavage in the duodenum. It shares the same catalytic triad with the structurally related endopeptidases trypsin and α-chymotrypsin, but

due to its small binding pocket cuts its substrates, mainly casein and elastin, only after small uncharged residues like alanine. Its high pI value of 8.7 and pH optimum at 8.0 suggests strong binding to anionic polymers; it was therefore very frustrating that even at pH 8.0 none of the 50 polymers was an effective inhibitor. Inspection of elastase's crystal structure[32] gives two hints for a plausible explanation: no basic or acidic residue is found in the direct vicinity of the active site; and many arginines and lysines are located close to aspartates and glutamates, facilitating internal ion pair formation which hinders complexation by an ionic external binder (**Scheme 3A**).

This is different with **α-chymotrypsin** (PDB code 1AFQ),[33] which is also proteolytically activated by trypsin in the duodenum. The enzyme also possesses a high pI value of 8.7 and a pH optimum of 7.8, but it cuts selectively after aromatic amino acids due to its spacious S1 pocket. In our polymer screen only very few polymers were efficient inhibitors. Contrary to our expectation these were cationic and carried benzamidine or guanidiniocarbonylpyrrole binding sites, which were combined with extended aromatic or aliphatic nonpolar arms. Intriguingly, there is a patch of two phenylalanines with two adjacent acidic residues directly next to α-chymotrypsin's active site, whereas most basic resides are located on the back side of the protein (**Scheme 3B**).[34]

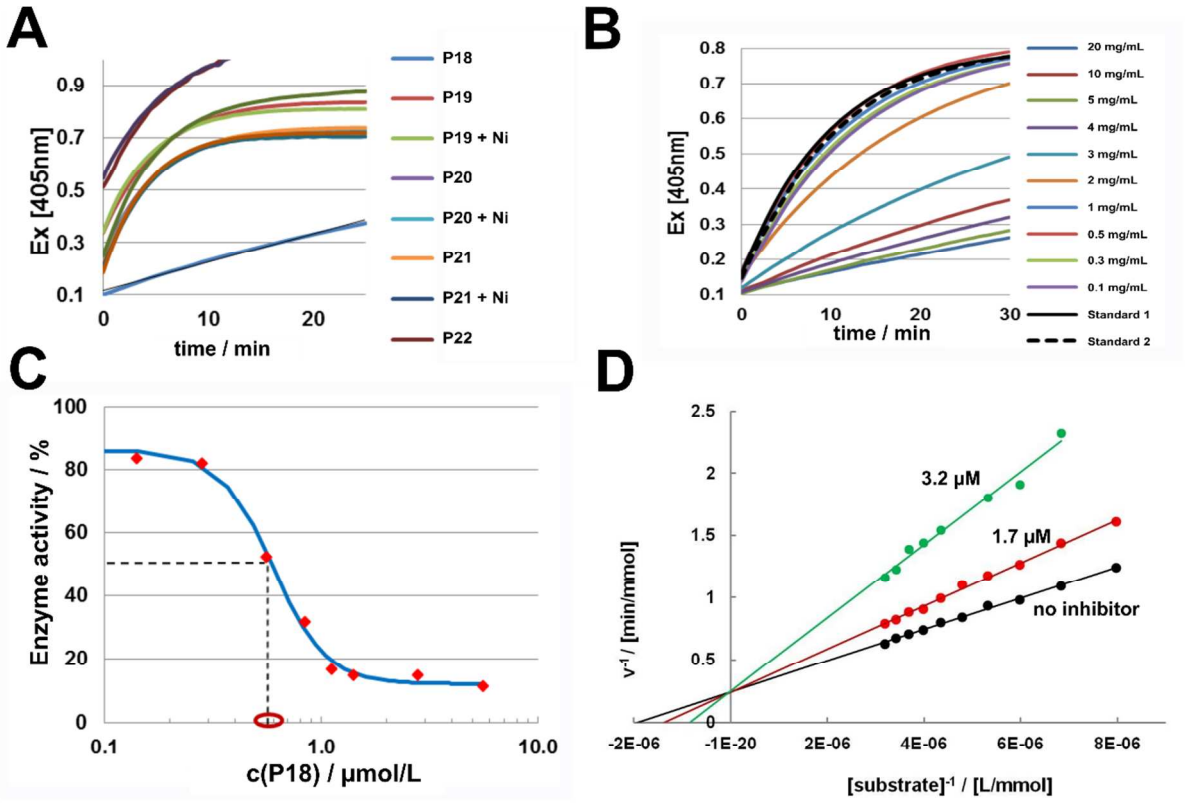

Figure 3. Polymer screening assay for determining IC_{50} values of the active compounds, illustrated for trypsin inhibition. **A** Only P18 is active; **B** Dose-dependent trypsin inhibition by P18; **C** Determination of the IC_{50} value for P18 (0.5 μM); **D** Lineweaver-Burk plot indicating competitive inhibition.

From a medicinal point of view, **trypsin**[35] (PDB code 4I8G–4I8L, 1S0R), is the most interesting serine protease, since it activates numerous other proteolytic enzymes and its overexpression and premature activation may ultimately be responsible for multiple organ damage. Trypsin is formed in the exocrinic pancreas part, and activated by autocatalysis in the duodenum. The strongly basic enzyme (pI 10.0) is especially rich in lysines and operates at a pH optimum between 7.5 and 8.5. Contrary to α-chymotrypsin, trypsin cuts after arginine and lysine. Various polymers turned out to be good to excellent trypsin inhibitors. They all contained the bisphosphonate arginine binder. However, the simultaneous presence of a small amount of boronic acid binders again lowered the IC_{50} value 6-fold. Indeed, trypsin contains 34 serines, which represent the most abundant residues (**Scheme 3C**). Serines in close proximity will readily form covalent cyclic boronate esters in a reversible manner.[36]

A similar effect was achieved by adding small amounts of NTA head groups. Surprisingly, the NTA groups increased affinity in the absence of Ni^{2+} ions, whereas especially the NTA homopolymer **P42** (but also the related **P43**) completely lost all their inhibitory power after equimolar Ni^{2+} addition. These results strongly indicate that histidine complexation is not the driving force behind the NTA/protein interaction. It seems as transition metal complexation even masks the NTA trianion – leaving a direct electrostatic attraction of lysine cations as the most probable interaction. The same phenomenon was already observed with efficient IgG complexation by NTA-rich polymers, and led to the discovery of a direct interaction between NTA head groups and lysine pairs on the surface of basic proteins.[12] It could be corroborated by ITC measurements (**Fig. 4**):[37] in a titration experiment trypsin was bound by the NTA homopolymer at a 2:1 stoichiometry (protein/polymer) in an enthalpically driven process (ΔH = -7.3 kcal/mol) with a small entropic cost ($T\Delta S$ = -1.7 kcal/mol). The resulting polymer protein affinity is relatively low (ΔG = -5.5 kcal/mol ~ 100 μM K_d). In the presence of 50 mol-% of Ni^{2+} ions, no binding isotherm could be obtained. Control experiments proved that Ni^{2+} ions as well as NTA monomers did not display any protein affinity, ruling out any unspecific metal/protein interactions and confirming a direct electrostatic NTA protein attraction. The fact that lysines are only complexed in the absence of Ni^{2+} ions, however strongly suggests, that the metal complex is thermodynamically more stable. If this is true, Ni^{2+} ions should be able to compete with a preformed enzyme NTA homopolymer complex. This was indeed observed when the saturated polymer enzyme complex was titrated against an equimolar solution of Ni^{2+} ions – in a competitive exothermic process the Ni^{2+} ions displaced the NTA homo polymer from the protein and formed the more stable Ni^{2+}/NTA complex.

If the affinity polymers bind to critical amino acids around the active site, they may inhibit enzyme activity by blocking the substrate access. In an exemplary case study, enzyme kinetics

for trypsin inhibition by **P52** were investigated and evaluated by Lineweaver-Burk plots (**Figure 3D**). Here the kinetic graphs for the enzyme in the absence and presence of increasing amounts of inhibitor polymer indeed had a common intersection with the ordinate, clearly indicating a competitive mechanism with reference to the substrate. In this case, the polymer competes with the substrate to be bound on the protein surface. Most likely, this is achieved, when the polymer sterically blocks the entrance to the active site.

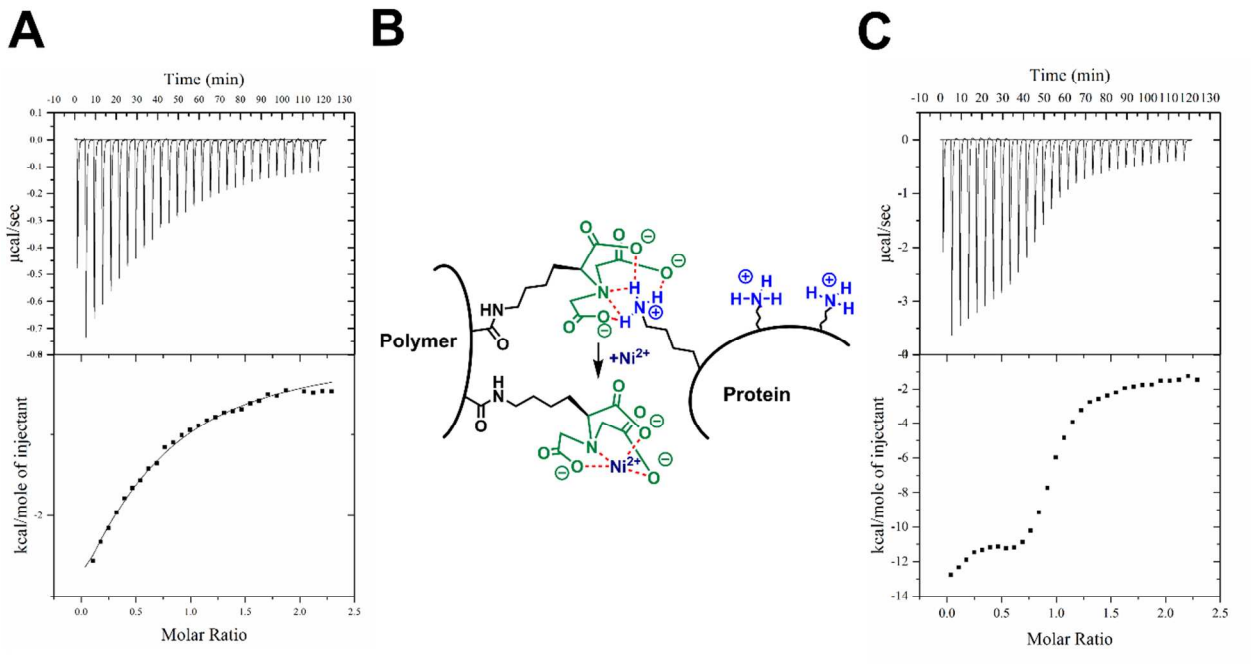

Figure 4. A Exothermic ITC titration of trypsin with increasing amounts of NTA homopolymer **P42**. **B** Lysine complexation by the NTA head in the absence of Ni^{2+} ions. **C** Back titration of the protein/polymer complex with Ni^{2+} ions is also enthalpy-driven because the stable NTA/Ni^{2+} complex is formed and the protein is released.

A good example for an acidic protease is **carboxypeptidase A** (PDB code 1F57, 5CPA).[38] It is a metalloprotease with a catalytically active Zn^{2+} ion and, like the serine proteases, it is activated by trypsin cleavage in the duodenum. Its pI is 6.0 with a pH optimum at 7.5. A large hydrophobic pocket accommodates both aromatic or aliphatic amino acid side chains. The Zn^{2+} ion together with an arginine activates the amide bond by Brønsted as well as Lewis acid catalysis and together with a glutamate helps to deprotonate a water nucleophile. Again, very few polymers were able to inhibit this metalloprotease. They all contain prominent NTA groups, but do not all require Ni^{2+} ions for shutting down the enzyme. The crystal structure shows several histidines, two pairs in or close to the active site (Scheme 3D).[39] Thus, direct interaction with the

catalytically active Zn^{2+}- histidine diad by NTA complexation at Zn^{2+} or even transmetallation by the polymer NTA-Ni^{2+} moieties may be the key interaction to interrupt enzyme activity. The presence of several bisphosphonate dianions will help to attach the polymer around the active site which is surrounded by multiple lysines, whereas most acidic residues are located on the back side of carboxypeptidase A. This may explain why no cationic polymers inhibit the acidic protease.

Kallikrein[40] (PDB code 5TJX, 1SPJ) is a very interesting case, because this serine protease is important in the early stage of the blood coagulation cascade. It is formed in the hepatozytes of the liver and is again activated by trypsin, but also by Factor XII (Hagemann factor). Kallikrein also operates in tissues and releases kinins, tissue hormones with general relevance in inflammatory processes. It is a strongly acidic enzyme with a pI of 4.0 - 4.5 and a pH optimum at 7-8. Contrary to expectations, again no cationic polymer was able to interfere with peptide cleavage by kallikrein. A relatively large number of BP and NTA-containing polymers however, turned out to be potent inhibitors, with a substantial overlap in the group of previously identified powerful trypsin inhibitors. In the crystal structure[41] two histidines are located on opposite ends at the entrance of the active site, whose complexation with a single NTA-rich polymer strand would entirely block the substrate approach (**Scheme 4A**). The active site is also surrounded by four serines, explaining the potency of two boronic acid-based polymers. Interesting enough, most glutamates and aspartates are located on the back side of kallikrein, leaving a lysine-rich patch underneath the active site. Most likely, this explains the inhibitory power of BP and NTA-rich polymers, even in the absence of Ni^{2+} ions.

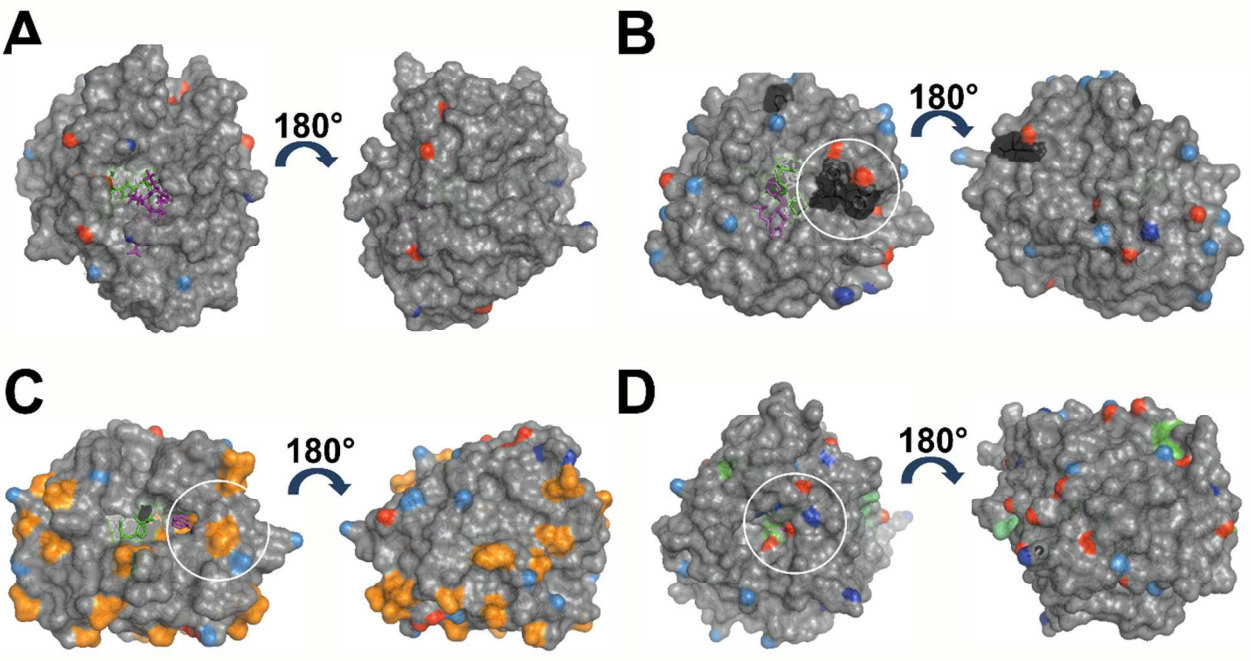

Scheme 3. Crystal structure of **A** pancreas elastase, **B** α-chymotrypsin, **C** trypsin and **D** carboxypeptidase A. Red spots represent carboxylate groups of acidic amino acids (Asp, Glu). Light blue spots indicate ammonium groups from lysines and dark blue spots arginines' guanidinium cations. The violet molecule is an inhibitor occupying the active site. The catalytic triad is depicted in green. Black areas are surface-exposed phenylalanines. Orange areas are surface-exposed serines. Green areas show histidines – turquoise are histidine pairs.

The most interesting feature of kallikrein inhibition by our affinity polymers, however, is their drastically sub-stoichiometric nature: 0.5 μM enzyme solutions were effectively inhibited at 3-12 nM polymer concentrations, corresponding to enzyme:polymer ratios of up to 190:1. For steric reasons, even polymers with a molecular weight of 100 kD are not able to complex such a large number of enzyme molecules at the same time. Digestion of the polymers to small oligomers or monomers is very unlikely because of their all-carbon backbone and can further be ruled out, since those small entities had no inhibitory effect on kallikrein. The underlying cause for this interesting sub-stoichiometric enzyme inhibition will be investigated in the near future.[42]

In order to avoid unwanted interference with blood coagulation, an orthogonal inhibition mode towards **Thrombin**[43-44] (PDB code 1A2C,1A3B) is especially important. This hydrolase is formed in the liver and activated during the blood coagulation cascade by factors Xa and Va. It exerts a fourfold arginine-glycine cleavage and thus activates fibrinogen to fibrin, which ultimately forms the thrombus. Thrombin is inhibited by antithrombin III, a process of fundamental importance for fibrinolysis (thrombus dissolution). The enzyme has a pI of 7.2 and a pH optimum of 7.5-8.5.

Only a few BP-rich copolymers were able to inhibit thrombin; and these required usually high polymer/protein excesses of up to 50 equivalents. Moreover, inhibition was limited to around 70%. There are some arginine and lysine clusters on thrombin's protein surface which will represent anchor points for the bisphosphonate units (**Scheme 4B**).[45] Contrary to many other hydrolases, NTA-rich polymers have no effect on thrombin activity. However, the presence of nonpolar binding sites such as dansyl or dodecyl within a polymer rich in bisphosphonates significantly lowers its IC_{50} value. A large hydrophobic patch stretches along one flank of the active site – well suited for hydrophobic and dispersive interactions.

Our final example, **Cathepsin D**,[46-47] represents a lysosomal aspartate endopeptidase (PDB code 1LYA, 4OBZ). Preprocathepsin D is formed in the rough endoplasmatic reticulum (ER) and converted by proteolytic cleavage and glycosylation to procathepsin D, which is then autocatalytically activated. A catalytic diad is formed by two aspartate residues, only one of which is protonated. Together, they deprotonate a nucleophilic water molecule, cut between two phenylalanines and protonate the released amide anion. Cathepsin is a markedly acidic protease, and operates at a pH range of 3.5-5 (**Scheme 4C**). In the assay, a self-quenched coumarin labeled decapeptide releases the fluorophore in a *turn-on* process and provides a highly sensitive detection mode.

It has to be taken into consideration that at a pH below 4 most carboxylates on cathepsine's surface[48] will be protonated, and only weakly bound by cationic polymers. However, di- and trianionic BP and NTA head groups are able to form a network of ionic hydrogen bonds towards these -CO_2H groups. It is hence not surprising, that most BP- and NTA-containing polymers were inhibitors of Cathepsin D with IC_{50} values in the low nanomolar range. Importantly, the single BP and NTA monomers had no inhibitory effect in the screening, ruling out that hydrolytic polymer cleavage might have produced small monomeric inhibitors.

Affinities and Selectivities. With the full account of all polymer/protein interactions at hand, a synoptic comparison of all polymers with respect to their protein selectivities becomes possible. Our results are summarized in **Table 3**. Each blank represents a polymer whose inhibitory power is at least 100 times weaker than that of all other inhibitors for a given enzyme. It should be emphasized that the overall enzyme concentrations in all assays varied between 2 nM and 2 µM. Thus the efficiency/effectivity of a polymer should not be measured by absolute IC_{50} values, but rather by comparison of the respective stoichiometric polymer/protein ratio. These values are always presented in the accompanying columns.

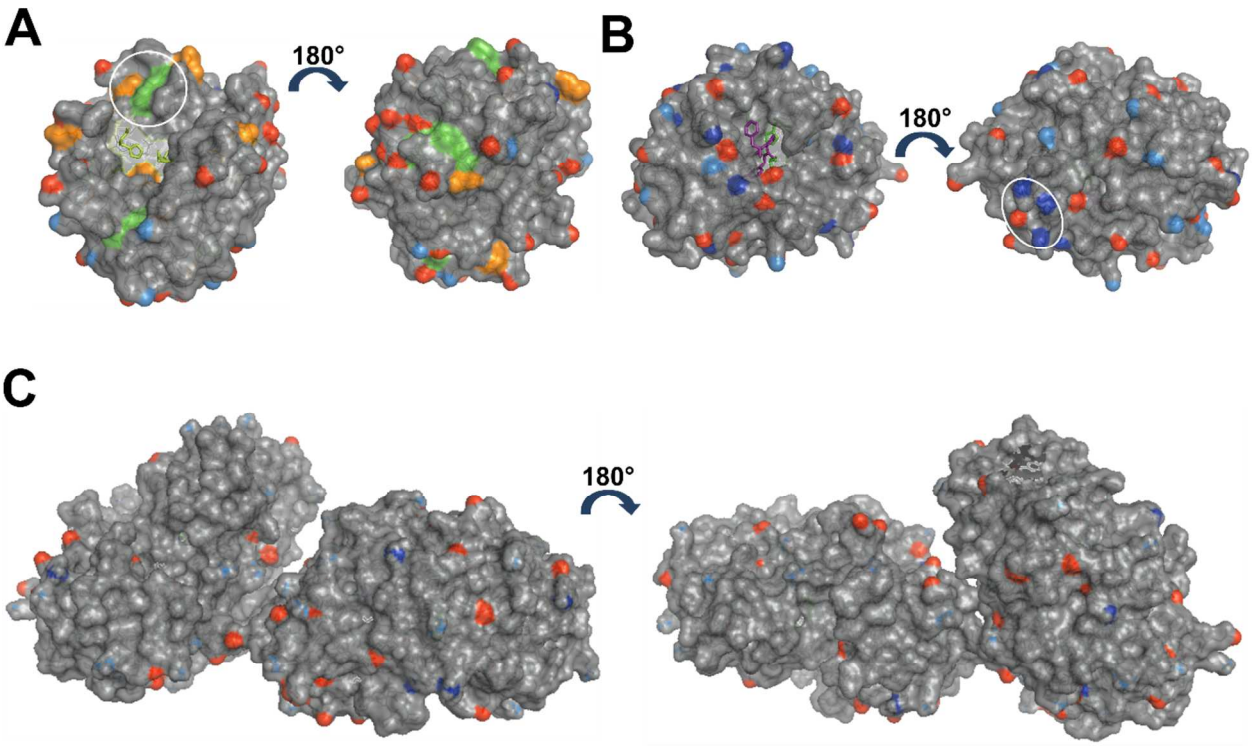

Scheme 4. Crystal structure of **A** kallikrein, **B** thrombin and **C** cathepsin D. Red spots represent carboxylate groups of acidic amino acids (Asp, Glu). Light blue spots indicate ammonium groups from lysines and dark blue spots arginines' guanidinium cations. The violet molecule is an inhibitor occupying the active site. The catalytic triad is green. Green areas show histidines – orange areas indicate serines.

In general, efficient inhibitors were found for all enzymes except for elastase. Quite often, the pI value of the protein is not a good guide for the choice of appropriately charged comonomers, because a majority of the complementary amino acid residues are located on the back of the protein, far away from the active site. On the contrary, for strong inhibition the direct environment around the active site seems to be critical. If a copolymer contains a significant amount of monomer units which bind directly next to the active site, it will efficiently prevent substrate access and product exit. This seems to be a very important factor that renders a given polymer a good enzyme inhibitor. In addition, a general affinity increase can be brought about by clusters of equally charged amino acids whose simultaneous interaction with an oppositely charged affinity polymer will lead to unspecific, but powerful attraction, which reaches far into the aqueous environment around the protein.

Table 3. Summary of all active polymers with their corresponding IC_{50} values and enzyme/polymer stoichiometries. Bold fields indicate the most protein-selective copolymer.

Polymer	α-Chymo-trypsin	Enzyme/ Polymer	Trypsin	Enzyme/ Polymer	Carboxy-peptidase A	Kallikrein	Enzyme/ Polymer	Thrombin	Enzyme/ Polymer	Cathepsin D	Enzyme/ Polymer
P01					3.8µM	3.9nM	136:1			<0.1µM	
+Ni					2.8µM	7.1nM	75:1			<0.1µM	
P02					1.6µM	7.6nM	70:1			<0.1µM	
+Ni					3.8µM	9.7nM	55:1			<0.1µM	
P08					**3.6µM**					<0.1µM	
P18			0.6µM	1:0.3		7.6nM	70:1			<0.1µM	
P24	**0.44µM**	1:0.9						**110nM**	1:12		
P32			1.3µM	1:0.7		3.7nM	143:1	470nM	1:53	31nM	1:12
P34			2.3µM	1:4.6		2.8nM	189:1	30nM	1:3.3	<0.1µM	
P36			3.2µM	1:1.6		4.4nM	120:1	70nM	1:7.8	<0.1µM	
P39			1.0µM	1:0.5		4.6nM	115:1			<0.1µM	
+Ni			1.6µM	1:0.8		9.2nM	58:1			<0.1µM	
P40			1.4µM	1:0.7		6.2nM	85:1			<0.1µM	
P41						7.7nM	69:1	17nM	1:1.9	<0.1µM	
P42			0.5µM	1:1.0		3.3nM	160:1			<0.1µM	
+Ni					1.3µM	6.1nM	87:1			<0.1µM	
P43			0.9µM	1:1.8		8.9nM	60:1			<0.1µM	
+Ni						**11.5nM**	46:1			<0.1µM	
P44			0.9µM	1:1.8		6.5nM	82:1			<0.1µM	
P45			1.4µM	1:2.9		6.0nM	88:1			<0.1µM	
P46			**1.8µM**	1:3.6						<0.1µM	
P47			**1.7µM**	1:3.4						<0.1µM	
P48			**1.5µM**	1:3.0						<0.1µM	
P49			**1.5µM**	1:3.0						<0.1µM	
P50			**1.5µM**	1:3.0						<0.1µM	
P03										**<0.1µM**	
P04										**<0.1µM**	
P05										**<0.1µM**	
P06										**<0.1µM**	

c(E)	0.5µM	2.0 / 0.5µM	n.d.	0.53µM	9nM	2.5nM

Most enzyme/polymer combinations did not lead to any change in enzyme activity – a prerequisite for selectivity. In light of all the above results, it can be inferred that only few favorable comonomer combinations and ratios lead to multipoint binding of our linear copolymers around the active site. Except P24 all polymers interact with cathepsin D. Some polymers shut down four of all seven highly diverse proteases, most of them with a dominating BP content (P32, P34 and P36).

There is a strong overlap between copolymers which are active against the related serine proteases trypsin and kallikrein, and all carboxypeptidase inhibitors likewise stop kallikrein. However, some affinity polymers are unique: thus P03-P06 selectively block cathepsin D. P24 only attenuates chymotrypsin and thrombin, and P08 selectively shuts down carboxypeptidase A (and cathepsin D). Similarly, P46-P50 block only trypsin (and cathepsin D), whereas P42 is active against carboxypeptidase A and kallikrein (as well as cathepsin) in the presence of Ni^{2+} ions. Finally, P41 targets kallikrein, thrombin (and cathepsin D).

In this protein series, monomers with medium-sized spacers (C_5/C_6) between their binding site and the methacrylamide moieties did not perform differently to their short counterparts without the spacer. We conclude that enough flexibility is maintained in the copolymers due to the presence of glucose "dummy" monomers. Even if the synthetic binding site (e.g., BP) is attached close to the polymer backbone, it is able to reach its complementary amino acid functionality on the protein surface (e.g., Lys/Arg). It remains to be examined whether or not the intense induced fit process of a linear copolymer on the complex protein surface, which ultimately leads to optimized multivalent and heteroavidic recognition, requires time and lowers entropy significantly.

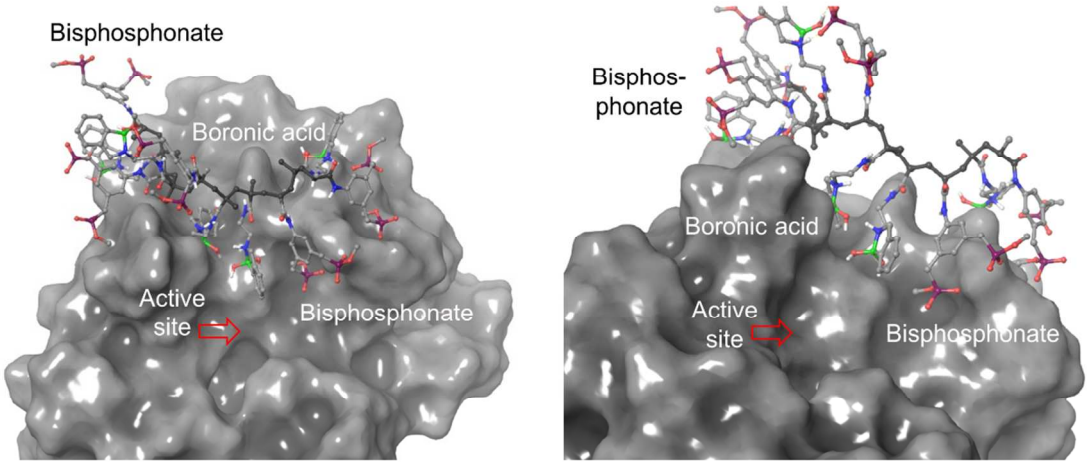

Figure 5. Visualization of a representative polymer fragment taken directly from polymer **P18** (ball and sticks) on bovine trypsin (Connolly surface). The picture shows several bisphosphonate units engaged in

chelate complexes with lysines and boronic acid moieties which formed covalent ester links to serines. (MacroModel 9.9, OPLS-2005, water/GBA solvation, MM calculation 10000 steps).

Several polymers with nonpolar comonomers were among the most efficient protease inhibitors. We tentatively explain this with the fast homopolymerization kinetics of the nonpolar reference comonomer, pointing to a potential formation of nonpolar polymer blocks which target extended nonpolar patches on a protein surface and thus contribute to high affinity binding.

Taken together, the synopsis in Table 3 reveals strengths and weaknesses of the underlying concept: various enzymes with similar active sites can be effectively distinguished by polymeric surface binders; and relative small variations in monomer composition greatly alter the inhibition potential and selectivity of these polymers. However, only a limited number of monomer binding sites contributes to strong binding; in particular, less polar monomers must be more efficiently isolated within the copolymer strand so that they can help to discriminate the immediate environment around a given active site.

For a visualization of the polymer binding mode on the protein surface we calculated the structure between a polymer fragment taken directly from **P18** and bovine trypsin (**Fig. 5**). After placing the polymer fragment closely above the trypsin surface next to the active site, a force-field calculation reached a minimum which shows several polymer binding sites engaged in specific interactions with the complementary amino acid residues; other polymer binding sites point away from the protein into the aqueous solvent. It should be taken into consideration, that this is only one possible snapshot out of many conformations due to the highly dynamic nature of the protein/polymer interaction.

Conclusion and Outlook. This account presents a general method for the construction of polymeric surface binders for digestion enzymes. Two prominent parts, namely the modification of the copolymer composition and the screening assay for the most powerful inhibitors are both amenable to parallelization. The concept hinges on the appropriate selection of amino-acid-selective comonomers, their free radical copolymerization, and subsequent screening of the resulting copolymer library for efficient enzyme inhibition. A microscale synthetic procedure for the copolymerization process was developed, which produces water-soluble affinity polymers that can be stored for years at room temperature. Initial parallel screening was conducted in standard enzyme assays to identify polymeric inhibitors, which were subsequently subjected to determination of IC_{50} values for their target enzyme. For all digestion enzymes except elastase a number of polymer inhibitors were found, some of which were selective towards one or two protein targets. Since the key monomers of the best inhibitors bind to amino acid residues in the direct vicinity of the active site, we conclude that efficient coverage of its immediate environment by the copolymers is critical. Strong interference with enzymatic activity is brought about by blocking the substrate access and product exit to and from the active site.

In the future we will further study the postulated inhibition mechanism in more detail, in order to find out how the extended linear affinity polymer explores the protein surface and leads to efficient enzyme inhibition. A special emphasis will be placed on the unexpected substoichiometric action of polymer inhibitors towards kallikrein. The most efficient and selective affinity polymers of this study will be subjected to toxicity and activity tests in isolated segments of rat intestines, and finally in animal models by collaboration partners at the university clinics. Since no membranes have to be passed to reach the intestinal walls, we propose oral administration of potential drugs in the final phase. The concept presented here may also be applied to the blood coagulation cascade or other essential multi-protein processes/pathways.

ASSOCIATED CONTENT.

Electronic supplementary information (ESI) available free of charge: Synthetic Procedures to monomers and polymers, NMR spectra, SEC spectra, calibration and reference curves for the enzyme assays, kinetics screening, dose-response plots for IC_{50} determination, Copolymerization kinetics (in NMR spectra), ITC titrations.

AUTHOR INFORMATION.

Corresponding Author

* E-mail: thomas.schrader@uni-due.de

Author Contributions

The manuscript was written through contributions of all authors. All authors have given approval to the final version of the manuscript.

Notes

The authors declare no competing financial interest.

ACKNOWLEDGMENT.

Financial support from the DFG-funded Collaborative Research Centre 1093 is gratefully acknowledged.

REFERENCES.

1. Schweizer, E.; Hoffmann-Röder, A.; Olsen, J. A.; Seiler, P.; Obst-Sander, U.; Wagner, B.; Kansy, M.; Banner, D. W.; Diederich, F., *Org. Biomol. Chem.* **2006,** *4*, 2364-2375.

2. Schmitt, L.; Tampé, R., *Prot. Eng.* Oxford Univ. Press UK: 1995.

3. Dernedde, J.; Rausch, A.; Weinhart, M.; Enders, S.; Tauber, R.; Licha, K.; Schirner, M.; Zügel, U.; von Bonin, A.; Haag, R., *PNAS* **2011,** *107*, 19679-19684.

4. Filby, M. H.; Muldoon, J.; Dabb, S.; Fletcher, N. C.; Ashcroft, A. E.; Wilson, A. J., *Chem. Commun.* **2011,** *47*, 559-561.

5. Yamaguchi, Y.; Kato, N.; Azuma, H.; Nagasaki, T.; Ohkanda, J., *Bioorg. Med. Chem. Lett.* **2012,** *22*, 2354-2358.

6. You, C.-C.; Miranda, O. R.; Gider, B.; Ghosh, P. S.; Kim, I.-B.; Erdogan, B.; Krovi, S. A.; Bunz, U. H. F.; Rotello, V. M., *Nat. Nanotechn.* **2007,** *2*, 318-323.

7. Sandanaraj, B. S.; Demont, R.; Aathimanikandan, S. V.; Savariar, E. N.; Thayumanavan, S., *J. Am. Chem. Soc.* **2006,** *128*, 10686-10687.

8. Lee, S.-H.; Hoshino, Y.; Randall, A.; Zeng, Z.; Baldi, P.; Doong, R.; Shea, K. J., *J. Am. Chem. Soc.* **2012,** *134*, 15765-15772.

9. Cutivet, A.; Schembri, C.; Kovensky, J.; Haupt, K., *J. Am. Chem. Soc.* **2009,** *131*, 14699-14702.

10. Zhang, H.; Jiang, J.; Zhang, H.; Zhang, Y.; Sun, P., *Macro Lett.* **2013,** *2*, 566-570.

11. Nishino, H.; Huang, C.-S.; Shea, K. J., *Angew. Chem. Int. Ed.* **2006,** *45*, 2392-2396.

12. Nematollahzedeh, A.; Sun, W.; Aureliano, C. S. A.; Lütkemeyer, D.; Stute, J.; Abdekhodaie, M. J.; Shojaei, A.; Sellergren, B., *Angew. Chem. Int. Ed.* **2001,** *50*, 495-498.

13. Canfarotta, F.; Poma, A.; Guerreiro, A.; Piletsky, S., *Nat. Prot.* **2016,** *11*, 443-455.

14. Turner, N. W.; Jeans, C. W.; Brain, K. R.; Allender, C. J.; Hlady, V.; Britt, D. W., *Biotechnol. Prog.* **2006,** *22*, 1474-1489.

15. Verheyen, E.; Schillemans, J. P.; van Wijk, M.; Demeniex, M.-A.; Hennink, W. E.; van Nostrum, C. F., *Biomaterials* **2011,** *32*, 3008-3020.

16. Renner, C.; Piehler, J.; Schrader, T., *J. Am. Chem. Soc.* **2006,** *128*, 620-628.

17. Koch, S.; Renner, C.; Xie, X.; Schrader, T., *Angew. Chem. Int. Ed.* **2006,** *45*, 6352-6355.

18. Wenck, K.; Koch, S.; Renner, C.; Sun, W.; Schrader, T., *J. Am. Chem. Soc.* **2007,** *129*, 16015-16019.

19. Latza, P.; Gilles, P.; Schaller, T.; Schrader, T., *Chem. Eur. J.* **2014,** *20*, 11479-11487.

20. Oldenburg, W. A.; Lau, L. L.; Rodenberg, T. J.; Edmonds, H. J.; Burger, C. D., *Arch. Intern. Med.* **2004,** *164*, 1054-1062.

21. Whitcomb, D. C., *New Engl. J. Med.* **2006,** *354*, 2142-2150.

22. Frossard, J. L.; Steer, M. L.; Pastor, C. M., *Lancet* **2008,** *371*, 143-152.

23. Uhl, W.; Buchler, M. W.; Malfertheiner, P.; Beger, H. G.; Adler, G.; Gaus, W., *Gut* **1999,** *45*, 97-104.

24. Buchler, M. W.; Malfertheiner, P.; Uhl, W.; Scholmerich, J.; Stockmann, F.; Adler, G.; Gaus, W.; Rolle, K.; Beger, H. G., *Gastroenterology* **1993,** *104*, 1165-1170.

25. Schmuck, C., *Chem. Eur. J.* **2000,** *6*, 709-718.

26. Hart, B. R.; Shea, K. J., *Macromolecules* **2002,** *35*, 6192-6201.

27. Lata, S.; Reichel, A.; Brock, R.; Tampé, R.; Piehler, J., *J. Am. Chem. Soc.* **2005,** *127*, 10205-10215.

28. Aguilar, M. R.; Gallardo, A.; del Mar Fernández, M.; San Román, J., *Macromolecules* **2002,** *35*, 2036-2041.

29. 2 mL Amicon Ultra 3K Membrane Filters, M. M.

30. Bergmeyer, H. U., 2nd ed.; Academic Press: New York, 1974; Vol. I.

31. Macdonald, S. J. F.; Dowle, M. D.; Harrison, L. A.; Clarke, G. D. E.; Inglis, G. G. A.; Johnson, M. R.; Shah, P.; Smith, R. A.; Amour, A.; Fleetwood, G.; Humphreys, D. C.; Molloy, C. R.; Dixon, M.; Godward, R. E.; Wonacott, A. J.; Singh, O. M. P.; Hodgson, S. T.; Hardy, G. W., *J. Med. Chem.* **2002,** *45*, 3878-3890.

32. Tamada, T.; Kinoshita, T.; Kurihara, K.; Adachi, M.; Ohhara, T.; Imai, K.; Kuroki, R.; T., T., *J. Am. Chem. Soc.* **2009,** *131*, 11033-11040.

33. Tsukada, H.; Blow, D. M., *J. Mol. Biol.* **1985,** *184*, 703-711.

34. Kashima, A.; Inoue, Y.; Sugio, S.; Maeda, I.; Nose, T.; Shimohigashi, Y., *Eur. J. Biochem.* **1998,** *255*, 12-23.

35. Liebschner, D.; Dauter, M.; Brzuszkiewicz, A.; Dauter, Z., *Acta Cryst.* **2013,** *69*, 1447-1462.

36. Transue, T. R.; Gabel, S. A.; London, R. E., *Bioconj. Chem.* **2006,** *17,* 300-308.

37. O'Brien, R.; Ladbury, J. E.; Chowdry, B. Z., Isothermal titration calorimetry of biomolecules. In *Protein-Ligand interactions: hydrodynamics and calorimetry*, Harding, S. E.; Chowdry, B. Z., Eds. Oxford Univ. Press: UK, 2000.

38. van Aalten, D. M. F.; Chong, C. R.; Joshua-Tor, L., *Biochemistry* **2000,** *39,* 10082-10089.

39. Jensen, A. F.; Bukrinsy, J. T.; Bjerrum, M. J.; Larsen, S., *Inorg. Chem.* **2002,** *7*, 490-499.

40. Li, Z.; Partridge, J. R.; Silva, A.; Rademacher, P.; Betz, A.; Xu, Q.; Sham, H.; Hu, Y.; Shan, Y.; Liu, B.; Zhang, Y.; Shi, H.; Ma, X.; Zhang, L., *ACS Med. Chem. Lett.* **2017**, *8*, 185–190.

41. Laxmikanthan, G.; Blaber, S. I.; Bernett, M. J.; Scarisbrick, I. A.; Juliano, M. A.; Blaber, M., *Proteins* **2005,** *58*, 802-814.

42. Evaluation of Enzyme Inhibitors in Drug Discovery: A Guide for Medicinal Chemists and Pharmacologists, Copeland, R. A., John Wiley & Sons: Hoboken, New Jersey, 2005.

43. Rios-Steiner, J. L. R.; Murakami, M.; Tulinsky, A., *J. Am. Chem. Soc.* **1998,** *120*, 597-598.

44. Skordalakes, E.; Elgendy, S.; Goodwin, C. A.; Green, D.; Scully, M. F.; Kakkar, V. V.; Freyssinet, J. M.; Dodson, G.; Deadman, J. J., *Biochemistry* **1998,** *37*, 14420-14427.

45. Biela, A.; Khayat, M.; Tan, H.; Kong, J.; Heine, A.; Hangauer, D.; Klebe, G., *J. Mol. Biol.* **2012,** *418*, 350-366.

46. Metcalf, P.; Fusek, M., *EMBO J.* **1993,** *12*, 1293-1302.

47. Gradler, U.; Czodrowski, P.; Tsaklakidis, C.; Klein, M.; Werkmann, D.; Lindemann, S.; Maskos, K.; Leuthner, B., *Bioorg. Med. Chem. Lett.* **2014,** *24*, 4141-4150.

48. Baldwin, E. T.; Bhat, T. N.; Gulnik, S.; Hosur, M. V.; Sowder II, R. C.; Cachau, R. E.; Collins, J.; Silva, A. M.; Erickson, J. W., *PNAS* **1993,** *90*, 6796-6800.

For Tables of Contents Use only

High-Affinity Copolymers Inhibit Digestive Enzymes by Surface Recognition

Patrick Gilles,[‡] Kirstin Wenck,[‡] Inga Stratmann,[‡] Michael Kirsch,[†] Daniel A. Smolin,[‡] Torsten Schaller,[‡] Herbert de Groot,[†] Arno Kraft,[§] Thomas Schrader[‡]*

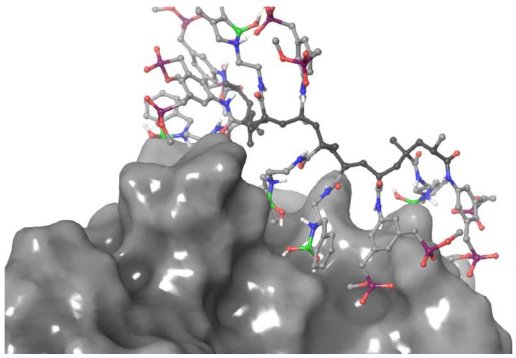

TOC graphics:

New affinity polymers recognize the surface of digestion enzymes, block the access to their active sites and thus stop enzyme activity.